



# Rescrutiny of the sansanmycin biosynthetic gene cluster leads to the discovery of a novel sansanmycin analogue with more potency against *Mycobacterium tuberculosis*

Yuanyuan Shi<sup>1,2</sup> · Xinwei Wang<sup>2</sup> · Ning He<sup>2</sup> · Yuning Xie<sup>2</sup> · Bin Hong<sup>1,2</sup>

Received: 14 June 2018 / Revised: 24 June 2019 / Accepted: 28 June 2019 / Published online: 24 July 2019  
© The Author(s), under exclusive licence to the Japan Antibiotics Research Association 2019

## Abstract

A novel sansanmycin analogue, sansanmycin Q (**1**), was identified by genome mining from the fermentation broth of *Streptomyces* sp. SS (CPC 200442). In comparison with other sansanmycin compounds, sansanmycin Q has an extra glycine residue at the N-terminus of the pseudopeptide backbone. The additional glycine was proved to be assembled to sansanmycin A by SsaB, a tRNA-dependent aminoacyltransferase, based on the results of rescrutiny of sansanmycin biosynthetic gene cluster, and then overexpression and knockout of *ssaB* in the wild-type strain. The structure of sansanmycin Q was assigned by interpretation of NMR and mass spectral data. The results of the bioassay disclosed that sansanmycin Q exhibited more potency against *Mycobacterium tuberculosis* H<sub>37</sub>Rv and a rifampicin- and isoniazid-resistant strain than sansanmycin A.

Sansanmycins, produced by *Streptomyces* sp. SS (CPC 200442) [1, 2], belong to the family of uridyl peptide antibiotics (UPAs) which also include pacidamycins [3, 4], mureidomycins [5, 6] and napsamycins [7]. They share a common structure, a 3'-deoxyuridyl attached via an unusual exocyclic enamide to a penta- or tetra-pseudopeptide backbone assembled by nonribosomal peptide synthetases (NRPSs). The UPAs target a clinically unexploited MrAY

(translocase I) to block the synthesis of the cell wall [8] and exhibit interesting antibacterial activity against highly refractory pathogens *Pseudomonas aeruginosa* and *Mycobacterium tuberculosis* [1, 9, 10]. UPAs have received considerable attention from synthetic chemistry and biosynthetic chemistry due to their unique structures, clinically yet-unexploited target and fascinating antibacterial activity.

Recently, it is proved that the tetra-pseudopeptide chain of UPAs is biosynthesized by NRPSs, and the extra alanyl residue at the N-terminus of the pentapeptide backbone in pacidamycin 1 and 3 (Fig. 1) is transferred by the tRNA-dependent aminoacyltransferase PacB from alanyl-tRNA to the N-terminus of the tetrapeptide intermediate [11–17]. PacB represents a new group of tRNA-dependent peptide bond-forming enzymes in secondary metabolite biosynthesis [17].

Although more than 20 sansanmycin analogues have been discovered until now, none of them are composed of a pentapeptide scaffold (Fig. 1) [1, 2, 18–21]. To get new sansanmycins with a pentapeptide backbone, we rescrutinized sansanmycin biosynthetic gene cluster, and a hypothetical protein SsaB with high homology to PacB was found. Then by LC–MS/MS analysis and LC–MS-directed purification, a new sansanmycin analogue with a pentapeptide backbone, sansanmycin Q (**1**), was obtained, and the function of SsaB was further confirmed in vivo by its overexpression and knockout. Herein, we report the isolation, structural elucidation and antibacterial activity of sansanmycin Q.

Yuanyuan Shi and Xinwei Wang contribute this work equally

**Supplementary information** The online version of this article (<https://doi.org/10.1038/s41429-019-0210-z>) contains supplementary material, which is available to authorized users.

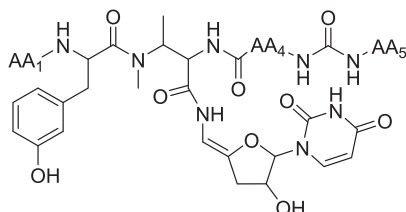
✉ Yuning Xie  
xieyy@imb.pumc.edu.cn

✉ Bin Hong  
binhong69@hotmail.com

<sup>1</sup> NHC Key Laboratory of Biotechnology of Antibiotics, Institute of Medicinal Biotechnology, Chinese Academy of Medical Sciences & Peking Union Medical College, Tiantanxili No.1, Beijing, China

<sup>2</sup> CAMS Key Laboratory of Synthetic Biology for Drug Innovation, Institute of Medicinal Biotechnology, Chinese Academy of Medical Sciences & Peking Union Medical College, Tiantanxili No.1, Beijing, China

In 2013, the biosynthetic gene cluster of sansanmycins was firstly identified and characterized in our lab [15, 16], which showed considerable sequence identity to the pacidamycin [15, 16] and napsamycin [15, 16] gene clusters. Within the gene cluster, SsaB shows 70% amino acid sequence identity and 81% similarity to PacB [17], along the whole length of the protein, which has been proved to transfer the alanyl residue to the N-terminus of pseudotetrapeptide. Besides, NpsN within the napsamycin gene cluster from *Streptomyces* sp. DSM 5940, and SrosN15\_15085 within the mureidomycin/napsamycin gene cluster from *Streptomyces*



| No. | Compounds      | AA <sub>1</sub> | AA <sub>4</sub> | AA <sub>5</sub> |
|-----|----------------|-----------------|-----------------|-----------------|
| 1   | Sansanmycin Q  | Gly             | Met             | Trp             |
| 2   | Sansanmycin A  | H               | Met             | Trp             |
| 3   | Pacidamycin 1  | Ala             | Ala             | Trp             |
| 4   | Pacidamycin 3  | Ala             | Ala             | <i>m</i> -Tyr   |
| 5   | Mureidomycin C | Gly             | Met             | <i>m</i> -Tyr   |

Fig. 1 Selected uridyl peptide antibiotics

*roseosporus* NRRL 15998, are also highly homologous to PacB. Moreover, a three-dimensional structural homology search performed using the online programme HHpred [22], also showed that SsaB is similar to transferases such as FemX of *Weissella viridescens* [23] and FemA of *Staphylococcus aureus* [24], which used an aminoacylated tRNA as a substrate (FemX: Ala; FemA: Gly) in the peptidoglycan precursor biosynthesis [23, 24]. All of these proteins belong to GCN5-related N-acetyltransferase superfamily [25, 26], and SsaB is closely clustered with SrosN15\_15085 and NpsN and then with PacB (Fig. S1). Besides the alanyl residue at the N-terminus of pacidamycin 1 and 3, a Gly residue at the N-terminus of the pseudotetrapeptide was ever observed in mureidomycin C in its producing strain in 1989 [6], but not found in heterologous expression strain [27, 28]. These bioinformatic analysis results suggest that SsaB might act as a tRNA-dependent peptide bond-forming transferase as PacB, resulting in the production of pentapeptide sansanmycin analogues.

To test the presence of sansanmycin analogues with a pentapeptide scaffold, the fermentation broth of *Streptomyces* sp. SS was enriched by Sep-Pak® C<sub>18</sub> Cartridges (Waters) and analyzed by the LC-MS/MS system coupled with a LTQ XT ion trap mass spectrometer (Thermo Fisher Scientific), using negative-mode electrospray ionization. The results showed that while there was no peak at  $m/z$  933  $[M-H]^-$ , corresponding to the pentapeptide sansanmycin

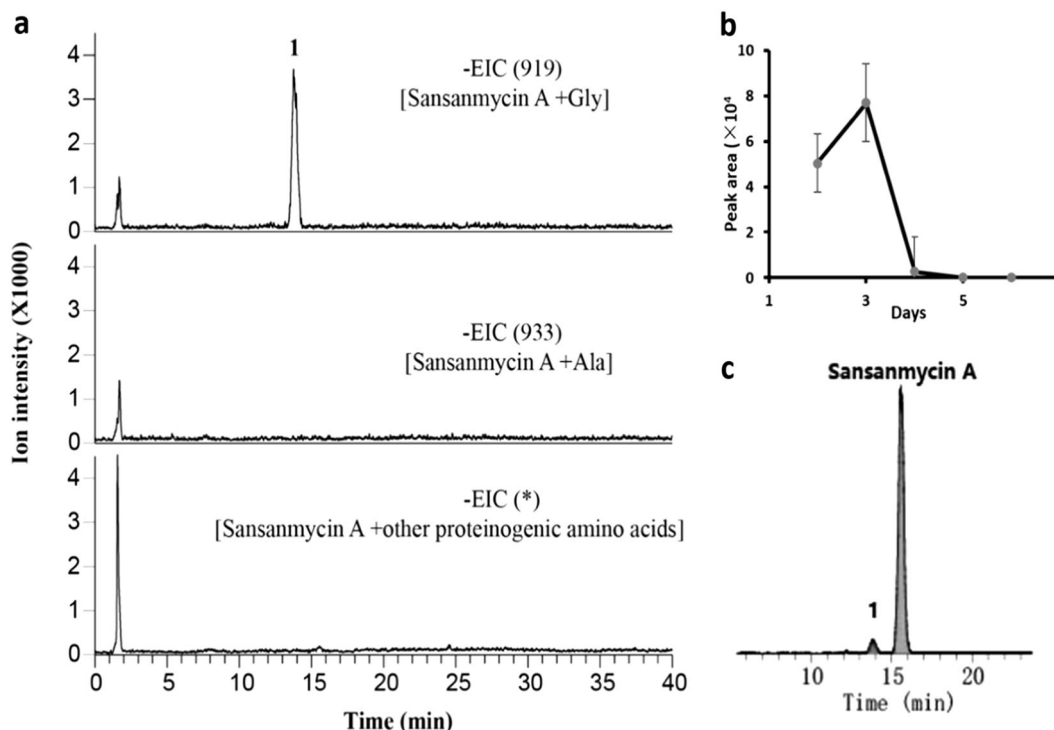


Fig. 2 Identification of sansanmycin analogues with a pentapeptide scaffold. **a** Extracted ion chromatograms showing the production of sansanmycin analogues with an extra amino acid residue. **b** The time-

dependent curve of the yield of compound **1**. **c** The relative yield of compound **1** and the major compound sansanmycin A on day 3 of fermentation

analogue bearing an alanine residue at the N-terminus, there was a peak (**1**) at  $m/z$  919  $[M-H]^-$ , which might correspond to pentapeptide sansanmycin analogues bearing a glycine (Fig. 2a). This potential compound was named as sansanmycin Q. Time-dependent production curves disclosed that the yield of sansanmycin Q in the wild-type strain reached the highest level on day 3 of the fermentation, then decreased dramatically on day 4 and disappeared since day 5 (Fig. 2b). In addition, the yield of sansanmycin Q was quite low, about 5% of that of the major compound sansanmycin A, even on day 3 (Fig. 2c).

To confirm that SsaB is responsible for adding the fifth amino acid to the N-terminus of sansanmycin A and to improve the yield of the corresponding product, *ssaB* was cloned and overexpressed in *Streptomyces* sp. SS. Complete *ssaB* coding region was cloned into a pSET152-derived expression plasmid, pL646 [29], to give the overexpression plasmid pL-*ssaB* (Fig. 3a). Then pL-*ssaB* was transferred into the wild-type strain by conjugation to get the *ssaB* overexpression strain SS/pL-*ssaB*, with pSET152-transferred strain SS/pSET152 as a control. Then these

recombinant strains were cultivated simultaneously, and the fermentation broth was enriched as above. The yield of sansanmycin Q was determined by the LC-MS/MS method. The LC-MS/MS is equipped with AB SCIEX Triple Quad™ 5500 mass spectrometer, which was operated in multiple-reaction monitoring mode, using the mass transition  $m/z$  921→717 for sansanmycin Q. The yield of sansanmycin Q in *ssaB* overexpression strain SS/pL-*ssaB* improved obviously than that in the control strain on the seventh day (Fig. 3b), which hinted that SsaB is involved in sansanmycin Q biosynthesis.

To further investigate the role of SsaB, the *ssaB* deletion strain (SS/BKO) was gained using PCR-targeting method as previously described (Fig. 3c) [17] and verified by PCR (Fig. 3d). Plasmid pL-*ssaB* was transferred into SS/BKO to get the complementary strain SS/BKO/pL-*ssaB*. Then all of the four different strains were cultivated simultaneously and the presence of sansanmycin Q in the fermentation broth on the fifth day was detected using LC-MS equipped with Agilent Triple Quad™ 6410 mass spectrometer in negative mode. The result (Fig. 3e) showed that sansanmycin Q was

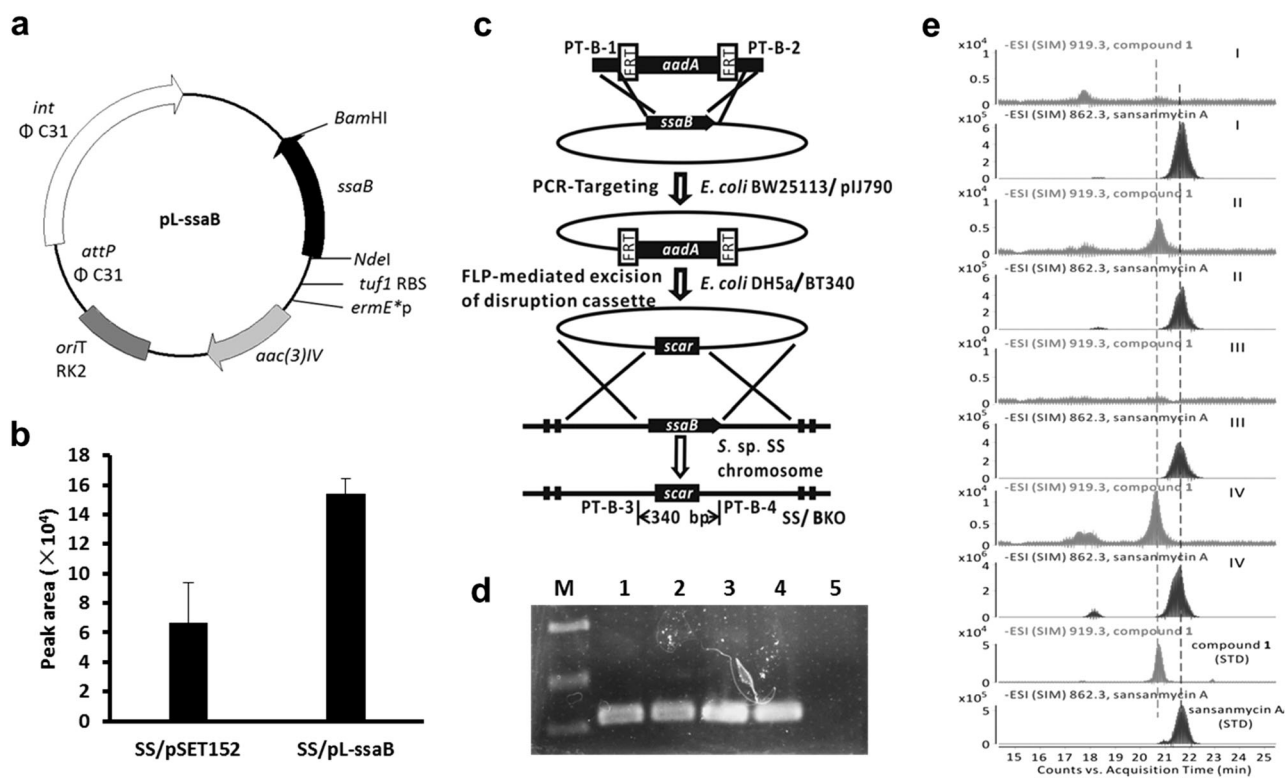


**Fig. 3** Overexpression and knockout of SsaB in *Streptomyces* sp. SS. **a** Schematic representation for construction of overexpression plasmid pL-*ssaB*. *int*, integrase from phage C31; *attP*, *attP* site from phage C31; *oriT*, *RK2* origin of single-stranded DNA transfer; *aac(3)IV*, apramycin resistance gene; *ermE*\*p, constitutive strong promoter; *tuf1* RBS, the sequence of the ribosomal binding site of Elongation Factor Tu1. **b** Comparison of the production of compound **1** in overexpression strain SS/pL-*ssaB* and control strain SS/pSET152 on the seventh day. The mass transition  $m/z$  921→717 was used. **c** Schematic

representation for construction of *ssaB* knockout mutant by PCR targeting. **d** The verification of SS/BKO by PCR analysis. Lane M: DNA ladder (800, 500 and 300 bp); lane 1–4: four conjugants of SS/BKO; lane 5: negative control. **e** Effects of the overexpression and knockout of *ssaB* on the production of compound **1** and sansanmycin A. I, SS/pSET152; II, SS/pL-*ssaB*; III, SS/BKO; IV, SS/BKO/pL-*ssaB*. The single ion monitor (SIM) of  $m/z$  919.3  $[M-H]^-$  was used for compound **1** (red line) and  $m/z$  862.3  $[M-H]^-$  was for sansanmycin A (blue line). STD represents standard compound (color figure online)

abolished in SS/BKO, while it existed in wild-type strain in trace. Furthermore, sansanmycin Q can be restored in SS/BKO/pL-ssaB. Based on the above results, it is further confirmed that SsaB is responsible for the biosynthesis of pentapeptide sansanmycin analogues in *Streptomyces* sp. SS.

Sansanmycin Q (**1**) was isolated and purified from *ssaB* overexpression strain SS/pL-ssaB according to the method described in the part of Materials and Methods (see the supporting information). Sansanmycin Q (**1**), isolated as white amorphous powder, showed the same UV spectrum as sansanmycin A (UV  $\lambda_{\max}^{\text{MeOH}}$  ( $\epsilon$ ): 258 (14129), 219 (27206)), and possessed a molecular formula  $\text{C}_{42}\text{H}_{52}\text{O}_{12}\text{N}_{10}\text{S}$  and 22° of unsaturation deduced from HRESIMS data ( $m/z$  921.35594  $[\text{M} + \text{H}]^+$  and  $m/z$  943.33990  $[\text{M} + \text{Na}]^+$ ), 47 mass units greater than that of sansanmycin A [1], which hinted at the presence of an extra glycine residue. Despite spectral complexities caused by rotational conformers, careful analysis of NMR ( $\text{D}_2\text{O}$ ) data for **1** (Table 1) still showed resonances for a carboxyl ( $\delta_{182.2}$ ), seven ester/amide carbonyls ( $\delta_{177.4}$ , 177.3, 176.0, 173.3, 170.4, 161.3, and 157.3), and eighteen  $sp^2$  carbons (Table 1), accounting for 17° of unsaturation and requiring that **1** incorporates five rings. By careful comparison with  $^1\text{H}$  NMR spectra of sansanmycin A<sup>1</sup>, that of compound **1** showed an extra signal at  $\delta_{3.26}$  (S, 2H), attributing to the presence of glycine. Further analysis of the  $^1\text{H}$ ,  $^{13}\text{C}$ , DEPT, COSY, HSQC and HMBC NMR spectroscopic data for **1** (Table 1) revealed signals and correlations, indicative of a 3'-deoxyuridyl and a penta-pseudopeptide composed of glycine, *m*-tyrosine, *N*-methyl-2,3-diaminobutyric acid (DABA), methionine and tryptophan.

The sequence of these fragments of **1** was proposed by the HMBC correlations (Fig. 4) and the MS/MS spectrum (Fig. 5). Firstly, the *N*-methyl proton ( $\delta_{\text{H}}$  3.03/2.63) and  $\alpha$  proton ( $\delta_{\text{H}}$  4.58/4.62) signals of DABA individually correlated to the carbonyl signals of *m*-Tyr ( $\delta_{\text{C}}$  176.0/175.4) and Met ( $\delta_{\text{C}}$  177.4), deducing the sequence of *m*-Tyr–DABA–Met. And the olefinic proton signal ( $\delta_{\text{H}}$  5.93/5.90) of 3'-deoxyuridyl showed a cross-peak to the carbonyl signal ( $\delta_{\text{C}}$  170.4/169.7) of DABA, indicative of 3'-deoxyuridyl attached to the carboxyl of DABA by an enamide. The downfield carbonyl signal ( $\delta_{\text{C}}$  182.2) of Trp compared to the other carbonyl signals indicated that Trp bears a free carboxyl group, deducing the location of Trp at the C-terminus of the penta-pseudopeptide. The carbonyl signal of Gly was observed at  $\delta_{\text{C}}$  177.3, suggesting that Gly is linked via an amide bond to *m*-Tyr. The fragment sequence of **1** was further confirmed by the ESIMS/MS data (Fig. 5). The fragment ion,  $m/z$  701, for the loss of Gly-*m*-tyrosine from N-terminus, further confirmed that the Gly locates at the N-terminus and is linked via a peptide bond to *m*-tyrosine. The fragment ions,  $m/z$  717 and 560,

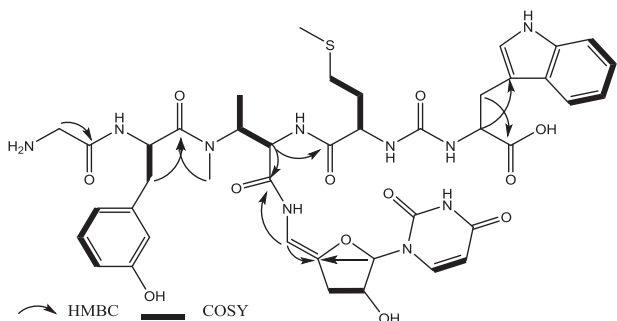
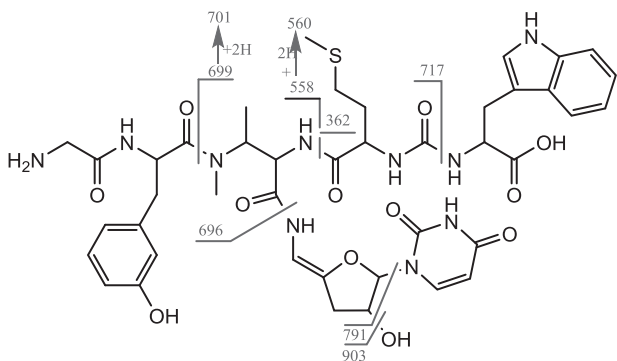
**Table 1**  $^1\text{H}$  NMR (600 MHz) and  $^{13}\text{C}$  NMR (150 MHz) data for sansanmycin Q (**1**)

| Position <sup>a</sup>  | Multiplicity      | $\delta_{\text{C}}$ | $\delta_{\text{H}}$ (J, Hz) | Extra signals due to conformers |                             |
|------------------------|-------------------|---------------------|-----------------------------|---------------------------------|-----------------------------|
|                        |                   |                     |                             | $\delta_{\text{C}}$             | $\delta_{\text{H}}$ (J, Hz) |
| Uracil-2               | N–CO–N            | 157.3               |                             |                                 |                             |
| Uracil-4               | CO–N              | 173.3               |                             |                                 |                             |
| Uracil-5               | CH                | 105.4               | 5.50, b                     |                                 | 5.81, b                     |
| Uracil-6               | CH                | 142.0               | 6.93, b                     |                                 | 7.27, b                     |
| Sugar-1                | O–CH–N            | 96.1                | 6.03, s                     | 96.5                            | 6.08, s                     |
| Sugar-2                | O–CH              | 75.4                | 4.23, m                     | 75.7                            | 4.52, m                     |
| Sugar-3                | CH <sub>2</sub>   | 35.8                | 2.84, m<br>2.88, m          |                                 | 2.63, m                     |
| Sugar-4                | >C=               | 147.1               |                             |                                 |                             |
| Sugar-5                | –CH=              | 99.5                | 5.93, s                     | 99.2                            | 5.90, s                     |
| DABA-1                 | CO–N              | 170.4               |                             | 169.7                           |                             |
| DABA-2                 | CH                | 58.3                | 4.58,<br>d (8.4)            | 58.9                            | 4.62,<br>d (8.4)            |
| DABA-3                 | CH                | 53.6                | 4.89, m                     | 56.8                            | 4.12, m                     |
| DABA-4                 | CH <sub>3</sub>   | 15.9                | 1.20,<br>d (6.6)            | 16.1                            | 0.63,<br>d (6.6)            |
| DABA–N–CH <sub>3</sub> | N–CH <sub>3</sub> | 32.9                | 3.03, s                     |                                 | 2.63, s                     |
| Met-1                  | CO–N              | 177.4               |                             |                                 |                             |
| Met-2                  | CH                | 55.9                | 4.23, m                     |                                 |                             |
| Met-3                  | CH <sub>2</sub>   | 33.6                | 1.89, b<br>1.80, b          |                                 |                             |
| Met-4                  | CH <sub>2</sub>   | 32.1                | 2.43, b                     |                                 |                             |
| Met–S–CH <sub>3</sub>  | CH <sub>3</sub>   | 17.0                | 2.02, s                     |                                 | 2.01, s                     |
| Ureido                 | N–CO–N            | 161.3               |                             |                                 |                             |
| Trp-1                  | –COOH             | 182.2               |                             |                                 |                             |
| Trp-2                  | CH                | 59.1                | 4.37, m                     |                                 |                             |
| Trp-3                  | CH <sub>2</sub>   | 31.1                | 3.26, m<br>3.08, m          |                                 |                             |
| Trp-2'                 | CH                | 127.0               | 7.19, s                     |                                 |                             |
| Trp-3'                 | ArC               | 113.3               |                             |                                 |                             |
| Trp-3a'                | ArC               | 130.2               |                             |                                 |                             |
| Trp-4'                 | ArCH              | 121.6               | 7.66, b                     |                                 |                             |
| Trp-5'                 | ArCH              | 121.9               | 7.13, m                     |                                 |                             |
| Trp-6'                 | ArCH              | 124.5               | 7.24, m                     |                                 |                             |
| Trp-7'                 | ArCH              | 114.5               | 7.46, b                     |                                 |                             |
| Trp-7a'                | ArC               | 138.9               |                             |                                 |                             |
| <i>m</i> -Tyr-1        | CO–N              | 176.0               |                             | 175.4                           |                             |
| <i>m</i> -Tyr-2        | CH                | 53.9                | 4.94, m                     |                                 | 5.16, m                     |
| <i>m</i> -Tyr-3        | CH <sub>2</sub>   | 39.4                | 2.92, m<br>2.67, m          |                                 | 2.93, m<br>2.84, m          |
| <i>m</i> -Tyr-1'       | ArC               | 140.8               |                             |                                 |                             |
| <i>m</i> -Tyr-2'       | ArCH              | 118.9               | 6.70, s                     |                                 |                             |
| <i>m</i> -Tyr-3'       | Ar–C–O            | 159.5               |                             |                                 |                             |
| <i>m</i> -Tyr-4'       | ArCH              | 117.3               | 6.75,<br>d (7.2)            |                                 |                             |
| <i>m</i> -Tyr-5'       | ArCH              | 133.0               | 7.18, m                     |                                 |                             |

**Table 1** (continued)

| Position <sup>a</sup> | Multiplicity    | $\delta_C$ | $\delta_H$ (J, Hz) | Extra signals due to conformers |                    |
|-----------------------|-----------------|------------|--------------------|---------------------------------|--------------------|
|                       |                 |            |                    | $\delta_C$                      | $\delta_H$ (J, Hz) |
| <i>m</i> -Tyr-6'      | ArCH            | 123.2      | 6.73, d (7.8)      |                                 |                    |
| Gly-1                 | –CO             | 177.3      |                    |                                 |                    |
| Gly-2                 | CH <sub>2</sub> | 46.1       | 3.26, s            |                                 |                    |

<sup>a</sup>Abbreviations for the structure units are *m*-Tyr *m*-tyrosine, Trp tryptophan, DABA *N*-methyl-2,3-diaminobutyric acid, Gly glycine, Met methionine

**Fig. 4** Selected COSY and HMBC correlations for **1****Fig. 5** ESIMS/MS data of parent ion ( $m/z$  921  $[M + H]^+$ ) of **1**

correspond to the loss of Trp and Met-ureido-Trp from C-terminus, respectively. The fragment ions,  $m/z$  903, 791 and 696, corresponding to the loss of H<sub>2</sub>O, H<sub>2</sub>O + uridyl and 3'-deoxyuridyl, respectively, confirmed the presence of the 3'-deoxyuridyl moiety.

The absolute configuration of sansanmycin Q (**1**) was tentatively determined on biogenetic grounds to be the same as its pacidamycin analogues, the absolute configuration of which has been established by total synthesis [30]. Methionine, *m*-tyrosine and tryptophan are of the natural, (*S*) configuration, and the DABA residue is of the (2*S*, 3*S*) configuration.

The obtained sansanmycin Q (**1**) was evaluated for its antibacterial activity against *P. aeruginosa* 11, *S. aureus*

**Table 2** Antibacterial effect of sansanmycin Q (**1**)

| Compounds     | MIC ( $\mu\text{g ml}^{-1}$ ) |                   |    |     |
|---------------|-------------------------------|-------------------|----|-----|
|               | H <sub>37</sub> Rv            | 2199 <sup>a</sup> | PA | SA  |
| Sansanmycin Q | 8                             | 8                 | 8  | >64 |
| Sansanmycin A | 16                            | 32                | 8  | >64 |
| Isoniazid     | 0.05                          | 40                | ND | ND  |
| Rifampicin    | 0.12                          | 20                | ND | ND  |

PA *P. aeruginosa* 11, SA *S. aureus* CCCC100051, ND not detected

<sup>a</sup>*M. tuberculosis* strain 2199 isolated from patients with tuberculosis in China was a rifampicin- and isoniazid-resistant strain

CPCC100051, as well as virulent *M. tuberculosis* strain H<sub>37</sub>Rv and isoniazid- and rifampicin-resistant strain 2199 which was isolated from patients with tuberculosis in China. The results disclosed that sansanmycin Q exhibited comparable activity against *P. aeruginosa* 11 with sansanmycin A, but 2–4-fold higher potency against H<sub>37</sub>Rv and isoniazid- and rifampicin-resistant strain 2199 than sansanmycin A (Table 2).

In this study, by rescrutinizing sansanmycin gene cluster, a novel uridyl peptide sansanmycin Q (**1**) with pentapeptide scaffold was identified from the fermentation broth of *Streptomyces* sp. SS (CPCC 200442). In comparison with the structure of sansanmycin A (**2**), sansanmycin Q (**1**) bears an additional glycine residue at the N-terminus of peptide backbone, which has been proved to be assembled to the N-terminus of the tetrapeptide of sansanmycin A by SsaB. Sansanmycin Q exhibits more potency against highly refractory pathogens *M. tuberculosis* (H<sub>37</sub>Rv and a rifampicin- and isoniazid-resistant strain) than sansanmycin A. To the best of our knowledge, it is the first time to report UPAs with pentapeptide backbone showed antimycobacterial activity. Although sansanmycin were modified by semi-synthesis method by our group [31] and dihydro-sansanmycin analogues were totally synthesized by Payne group [32], the complexity of its structure still brings great difficulties for further chemical modification. This finding of a more potent pentapeptide sansanmycin analogue points out a direction that the structures of UPAs can be simply modified by adding an amino acid residue to the N-terminus to obtain more diverse and potential analogues.

**Acknowledgements** We acknowledge financial support from the Drug Innovation Major Project (2018ZX09711001-006-011 and 2018ZX09711001-007-001), the National Natural Science Foundation of China (81803410, 81872780, 81273415, 81603007, 81630089 and 81621064), CAMS Innovation Fund for Medical Sciences (2016-I2M-3-012, 2016-I2M-2-002 and 2018-I2M-3-005), Beijing Natural Science Foundation (7172137 and 7184227), the Fundamental Research Funds for the Central Universities (3332018095) and Institute of Medicinal Biotechnology Foundation (2016ZX350045 and 2016ZX350053).

## Compliance with ethical standards

**Conflict of interest** The authors declare that they have no conflict of interest.

**Publisher's note:** Springer Nature remains neutral with regard to jurisdictional claims in published maps and institutional affiliations.

## References

- Xie Y, Chen R, Si S, Sun C, Xu H. A new nucleosidyl-peptide antibiotic, sansanmycin. *J Antibiot.* 2007;60:158–61.
- Xie Y, et al. NRPS substrate promiscuity leads to more potent antitubercular sansanmycin analogues. *J Nat Prod.* 2014;77:1744–8.
- Fronko RM, Lee JC, Galazzo JG, Chamberland S, Malouin F, Lee MD. New pacidamycins produced by *Streptomyces coeruleorubidus*, NRRL 18370. *J Antibiot.* 2000;53:1405–10.
- Chen RH, Buko AM, Whittern DN, McAlpine JB. Pacidamycins, a novel series of antibiotics with anti-*Pseudomonas aeruginosa* activity. II. Isolation and structural elucidation. *J Antibiot.* 1989;42:512–20.
- Isono F, Sakaida Y, Takahashi S, Kinoshita T, Nakamura T, Inukai M, Mureidomycins E. and F, minor components of mureidomycins. *J Antibiot.* 1993;46:1203–7.
- Isono F, Inukai M, Takahashi S, Haneishi T, Kinoshita T, Kuwano H, Mureidomycins A-D. novel peptidynucleoside antibiotics with spheroplast forming activity. II. Structural elucidation. *J Antibiot.* 1989;42:667–73.
- Chatterjee S, et al. Napsamycins, new *Pseudomonas* active antibiotics of the mureidomycin family from *Streptomyces* sp. HIL Y-82,11372. *J Antibiot.* 1994;47:595–8.
- Isono F, Inukai M. Mureidomycin A, a new inhibitor of bacterial peptidoglycan synthesis. *Antimicrob Agents Chemother.* 1991;35:234–6.
- Fernandes PB, et al. Pacidamycins, a novel series of antibiotics with anti-*Pseudomonas aeruginosa* activity. III. Microbiologic profile. *J Antibiot.* 1989;42:521–6.
- Isono F, Katayama T, Inukai M, Haneishi T, Mureidomycins A-D. novel peptidynucleoside antibiotics with spheroplast forming activity. III. Biological properties. *J Antibiot.* 1989;42:674–9.
- Rackham EJ, Gruschow S, Ragab AE, Dickens S, Goss RJ. Pacidamycin biosynthesis: identification and heterologous expression of the first uridyl peptide antibiotic gene cluster. *Chembiochem.* 2010;11:1700–9.
- Zhang W, Ostash B, Walsh CT. Identification of the biosynthetic gene cluster for the pacidamycin group of peptidyl nucleoside antibiotics. *Proc Natl Acad Sci USA.* 2010;107:16828–33.
- Zhang W, et al. Nine enzymes are required for assembly of the pacidamycin group of peptidyl nucleoside antibiotics. *J Am Chem Soc.* 2011;133:5240–3.
- Kaysser L, et al. Identification of a napsamycin biosynthesis gene cluster by genome mining. *Chembiochem.* 2011;12:477–87.
- Li Q, Wang L, Xie Y, Wang S, Chen R, Hong B. SsaA, a member of a novel class of transcriptional regulators, controls sansanmycin production in *Streptomyces* sp. strain SS through a feedback mechanism. *J Bacteriol.* 2013;195:2232–43.
- Wang L, et al. Draft genome sequence of *Streptomyces* sp. strain SS, which produces a series of uridyl peptide antibiotic sansanmycins. *J Bacteriol.* 2012;194:6988–9.
- Zhang W, Ntai I, Kelleher NL, Walsh CT. tRNA-dependent peptide bond formation by the transferase PacB in biosynthesis of the pacidamycin group of pentapeptidyl nucleoside antibiotics. *Proc Natl Acad Sci USA.* 2011;108:12249–53.
- Xie Y, Xu H, Si S, Sun C, Chen R. Sansanmycins B and C, new components of sansanmycins. *J Antibiot.* 2008;61:237–40.
- Xie Y, Xu H, Sun C, Yu Y, Chen R. Two novel nucleosidyl-peptide antibiotics: sansanmycin F and G produced by *Streptomyces* sp SS. *J Antibiot.* 2010;63:143–6.
- Shi Y, et al. Improving the N-terminal diversity of sansanmycin through mutasynthesis. *Microb cell Factor.* 2016;15:77.
- Zhang N, et al. Precursor-directed biosynthesis of new sansanmycin analogs bearing para-substituted-phenylalanines with high yields. *J Antibiot.* 2016;69:765–8.
- Alva V, Nam SZ, Soding J, Lupas AN. The MPI bioinformatics toolkit as an integrative platform for advanced protein sequence and structure analysis. *Nucleic Acids Res.* 2016;44:W410–5.
- Biarrotte-Sorin S, Maillard AP, Delettre J, Sougakoff W, Arthur M, Mayer C. Crystal structures of *Weissella viridescens* FemX and its complex with UDP-MurNAc-pentapeptide: insights into FemABX family substrates recognition. *Structure.* 2004;12:257–67.
- Benson TE, et al. X-ray crystal structure of *Staphylococcus aureus* FemA. *Structure.* 2002;10:1107–15.
- Neuwald AF, Landsman D. GCN5-related histone N-acetyltransferases belong to a diverse superfamily that includes the yeast SPT10 protein. *Trends Biochem Sci.* 1997;22:154–5.
- Vetting MW, et al. Structure and functions of the GNAT superfamily of acetyltransferases. *Arch Biochem Biophys.* 2005;433:212–26.
- Jiang L, et al. Identification of novel mureidomycin analogues via rational activation of a cryptic gene cluster in *Streptomyces roseosporus* NRRL 15998. *Sci Rep.* 2015;5:14111.
- Tang X, Gross M, Xie Y, Kulik A, Gust B. Identification of mureidomycin analogues and functional analysis of an N-acetyltransferase in napsamycin biosynthesis. *Chembiochem.* 2013;14:2248–55.
- Hong B, Phornphisutthimas S, Tilley E, Baumberg S, McDowall KJ. Streptomycin production by *Streptomyces griseus* can be modulated by a mechanism not associated with change in the adpA component of the A-factor cascade. *Biotechnol Lett.* 2007;29:57–64.
- Boojamra CG, et al. Stereochemical elucidation and total synthesis of dihydropacidamycin D, a semisynthetic pacidamycin. *J Am Chem Soc.* 2001;123:870–4.
- Li YB, et al. Synthesis and in vitro antitubercular evaluation of novel sansanmycin derivatives. *Bioorg Med Chem Lett.* 2011;21:6804–7.
- Tran AT, et al. Sansanmycin natural product analogues as potent and selective anti-mycobacterials that inhibit lipid I biosynthesis. *Nat Commun.* 2017;8:14414.